



Observational constraints for C-rich AGB stars

G. Rau¹, J. Hron¹, C. Paladini², B. Aringer³, P. Marigo³, and K. Eriksson³

- ¹ University of Vienna, Department of Astrophysics, Türkenschanzstrasse 17, A-1180 Vienna
e-mail: gioia.rau@univie.ac.at
- ² Institut d'Astronomie et d'Astrophysique, Université Libre de Bruxelles, Boulevard du Triomphe CP 226, B-1050 Bruxelles, Belgium
- ³ Department of Physics and Astronomy G. Galilei, Vicolo dell'Osservatorio 3, 35122 Padova, Italy

Abstract. We modeled the atmospheres of six carbon-rich Asymptotic Giant Branch stars (R Lep, R Vol, Y Pav, AQ Sgr, U Hya, and X TrA) using VLT/MIDI interferometric observations, together with spectro-photometric data, we compared them with self-consistent, dynamic model atmospheres. The results show that the models can reproduce the Spectral Energy Distribution (SED) data well at wavelengths longer than $1 \mu\text{m}$, and the interferometric observations between $8 \mu\text{m}$ and $10 \mu\text{m}$. We found differences at wavelengths shorter than $1 \mu\text{m}$ in the SED, and longer than $10 \mu\text{m}$ in the visibilities. The discrepancies observed can be explained in terms of a combination of data- and model-related reasons. We derived some stellar parameters, and our findings agree well with literature values within the uncertainties. Also, when comparing the location of the stars in the H-R diagram, with evolutionary tracks, the results show that the main derived properties (L , T_{eff} , C/O ratios and stellar masses) from the model fitting are in good agreement with TP-AGB evolutionary calculations.

Key words. instrumentation: high angular resolution – techniques: interferometric – stars: AGB and post-AGB – stars: atmospheres – stars: circumstellar matter – stars: fundamental parameters

1. Introduction

The final evolutionary stages of stars with initial masses from 0.8 to $8.0 M_{\odot}$ are characterized by a phase on the AGB (Habing & Olofsson, 2003). AGB stars are one of the major contributors to the chemical enrichment of galaxies. In particular, carbon stars provide amC & SiC dust, whose formation process is rather well understood (Höfner et al., 2003). However, we still lack observational constraints and consistent comparison with models.

In this contribution, we summarize part of the work done by Rau et al. (2015) and Rau et al. (2017), who derived atmospheric stratifications, fundamental stellar parameters, and dust properties of a sample of C-rich AGB stars. From these, we provided constraints for the dynamic model atmospheres used hereby (e.g. Fleischer et al., 1992; Höfner & Dorfi, 1997; Höfner et al., 2003), the mass loss process for carbon stars, and for stellar evolution models (e.g. Marigo et al., 2013, 2017).

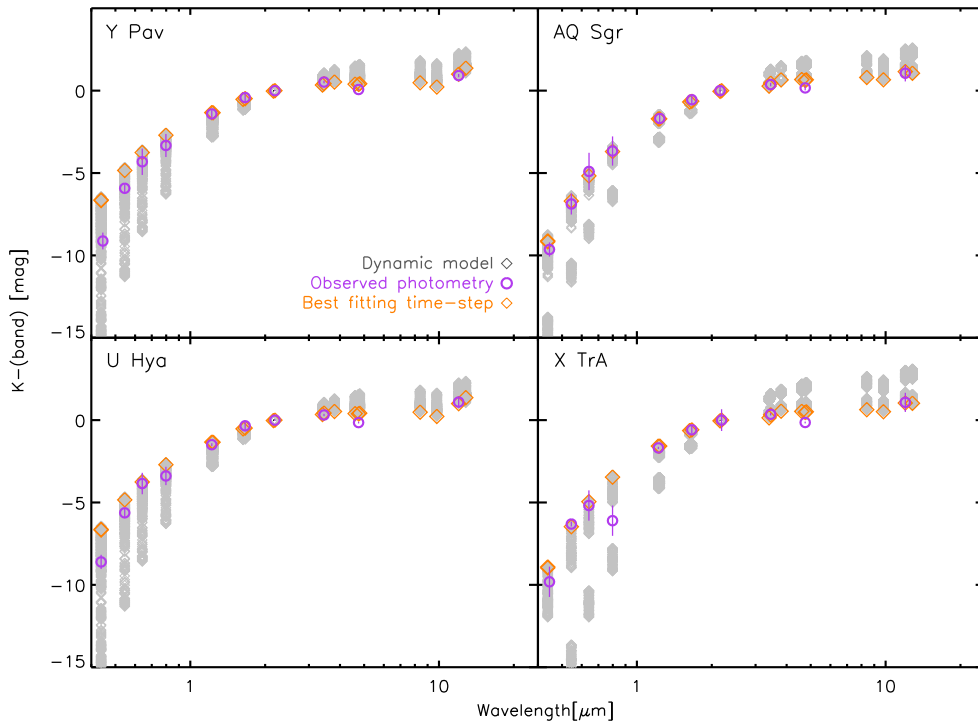


Fig. 1. Photometric observations of SRb and Lb stars: Y Pav (upper left) and AQ Sgr (upper right), and U Hya (lower left) and X TrA (lower right). Observations (violet circles) are compared to the dynamic model’s synthetic photometry (gray diamonds). Orange diamonds show the best fitting time-steps of the four stars.

2. Sample, data, and methods

Our sample (see Table 1 in Rau et al., 2017) consists of six carbon stars observed with VLT/MIDI, showing: (1) SiC feature; (2) no evidence of asymmetric structures in the N -band within the first few stellar radii (Paladini et al., 2017). Namely, those are: R Lep, R Vol, Y Pav, U Hya, AQ Sgr, X TrA.

We used photometric, spectroscopic, and interferometric data, which were fitted with geometric models (Klotz et al., 2012) and dynamic model atmospheres (Eriksson et al., 2014; Höfner et al., 2016). The photometric data in the B , V , R , I , J , H , $K L$, M , $N1$, $N2$, $N3$ and $IRAS12$ bands were taken from the literature. Also, for just one star presented in this work, R Lep, an IRTF spectrum (Rayner et al., 2009) that covers the wavelength range $\lambda = [0.8, 5.0] \mu\text{m}$ is available.

Interferometric observations with the MIDI instrument on the Very Large Telescope Interferometer (Leinert et al., 2003) were used. MIDI provides spectrally resolved visibilities, photometry and differential phases from 8 to 13 μm). We performed a fit of the photometry among the whole grid, deriving one best fitting model. The latter model served to calculate the synthetic visibilities, for each time-steps, for the subsequent interferometric fit. In Fig. 1 we show the results of the fit for the semiregular and irregular variables; for details and the interferometric fit, please refer to Rau et al. (2017).

2.1. Results and discussion

With respect to the results found by Rau et al. (2015), we found an improvement in the pho-

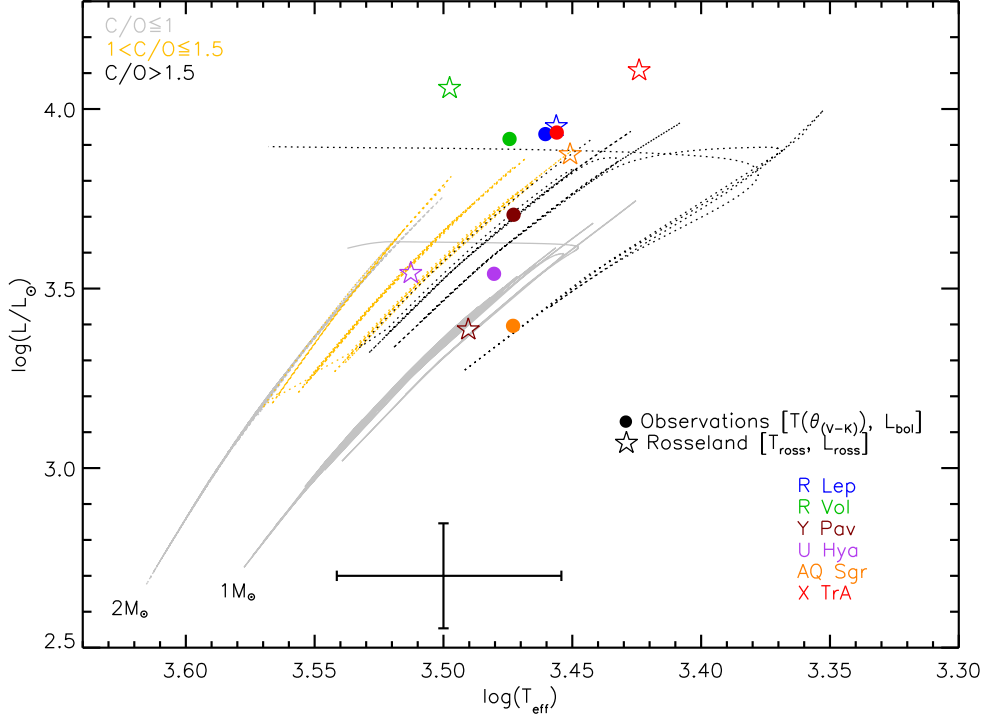


Fig. 2. AGB region of the H-R diagram. The lines display solar metallicity evolutionary tracks from Marigo et al. (2013): gray lines mark the regions of Oxygen-rich stars with $C/O < 1.0$; yellow lines denote the region of C-rich stars with $1.0 < C/O \leq 1.5$, while black lines mark stars with $C/O > 1.5$. The numbers indicate the mass values at the beginning of the thermal pulsing (TP)-AGB. For better visibility, the track with $2 M_{\odot}$ is plotted with a dotted line. Different symbols and colors refer to the luminosity and effective temperature, estimated through the comparison in this work of the models with spectro-photometric-interferometric-observations. A typical error-size bar is shown in the lower side of the figure.

tometric fitting, though with remaining differences at wavelengths shorter than $1 \mu\text{m}$, which we hypothesized to be due to a combination of data-related (in the meaning of lack of light curves), and model-related reasons (i.e. the assumption of Small Particle Limit (SPL), or due to the amC opacity). The differences between the synthetic visibilities and the observed ones longward than $10 \mu\text{m}$ are likely due to a smoother density distribution in the models w.r.t. the observations, to a clumpy environment, or to the possible influence of C_2H_2 and HCN contribution on the visibilities. We believe some discrepancies to be related instead to the SiC dust; SiC is added artificially a-posteriori in the dynamic models using the COMA code (Aringer, 2000; Aringer

et al., 2009), assuming that it condenses together with SiC. Thus, for a complete test of this problem, we have to await a modifications in the models in a similar way as currently done for M-type stars (Höfner et al., 2016).

We also derived stellar parameters, through a comparison of the stars parameters derived from the models and from our interferometric observations, with the evolutionary tracks from Marigo et al. (2013). From the dynamic models we derive the Rosseland diameter (θ_{Ross}), and the temperature of the time-step at this radius (T_{Ross}); from the photometric observations we obtained the bolometric luminosity L_{bol} , a diameter $\theta_{(V-K)}$, and an effective temperature $T(\theta_{(V-K)})$ using the diameter vs. $(V-K)$ relation of van Belle et al. (2013); while from

the interferometric observations we derived a Uniform Disk diameter at 8 and 12 μm . We compared those parameters within each other and we obtained that the parameters derived from spectro-interferometric observations are in good agreement with the ones derived from the dynamic models. Also, the location of all the observed stars in the H-R diagram (see Fig. 2) are in good agreement with the C/O ratio and M derived from the dynamic models, and is consistent with the part of the TP-AGB track (in Fig. 7, from Marigo & Aringer, 2009) that corresponds to the C-rich evolution.

3. Conclusions

We conclude that the atmospheres are extended with indications for shell-like structure, larger in the Miras than in Semiregular and Irregular stars. The SEDs show a discrepancy between synthetic and observed SED at wavelength shorter than 1 μm , while in the visibilities we observe a difference, between synthetic and observed visibility, in the visibility shape beyond 10 μm , and different amC opacities do not solve the visibilities slope effect below 10 μm , and do not affect the visibilities shape above. The stellar parameters are mostly in agreement with the evolutionary tracks, and the SiC profile shape is not well reproduced with Pegourie opacities. A coherent test will be possible only when the SiC condensation will be self-consistently included in the models.

Acknowledgements. GR thanks the conference organizers, Paolo Ventura, and the SOC, for having received the fee waiver, and the University of Vienna for having granted her the Abschlussstipendium. This work is supported by the Austrian Science Fund FWF under project number P23006-N16.

AB and PM acknowledge support by the ERC Consolidator Grant funding scheme (*project STARKEY*, G.A. n. 615604). PC acknowledge the support of the Belgian Fund for Scientific Research F.R.S.- FNRS. PC acknowledge the support of the Belgian Fund for Scientific Research F.R.S.- FNRS.

References

- Aringer, B. 2000, in *The Carbon Star Phenomenon*, ed. R. F. Wing (Kluwer, Dordrecht), IAU Symp. 177, 519
- Aringer, B., et al. 2009, *A&A*, 503, 913
- Eriksson, K., et al. 2014, *A&A*, 566, A95
- Fleischer, A. J., Gauger, A., & Sedlmayr, E. 1992, *A&A*, 266, 321
- Habing, H. J. & Olofsson, H. 2004, *Asymptotic giant branch stars* (Springer, New York)
- Höfner, S. & Dorfi, E. A. 1997, *A&A*, 319, 648
- Höfner, S., et al. 2003, *A&A*, 399, 589
- Höfner, S., Bladh, S., Aringer, B., & Ahuja, R. 2016, *A&A*, 594, A108
- Klotz, D., Sacuto, S., Paladini, C., Hron, J., & Wachter, G. 2012, *Proc. SPIE*, 8445, 84451
- Leinert, C., Graser, U., Richichi, A., et al. 2003, *The Messenger*, 112, 13
- Marigo, P. & Aringer, B. 2009, *A&A*, 508, 1539
- Marigo, P., et al. 2013, *MNRAS*, 434, 488
- Marigo, P., Girardi, L., Bressan, A., et al. 2017, *ApJ*, 835, 77
- Paladini, C., Klotz, D., Sacuto, S., et al. 2017, *A&A*, 600, A136
- Rau, G., Paladini, C., Hron, J., et al. 2015, *A&A*, 583, A106
- Rau, G., Hron, J., Paladini, C., et al. 2017, *A&A*, 600, A92
- Rayner, J. T., Cushing, M. C., & Vacca, W. D. 2009, *ApJS*, 185, 289
- van Belle, G. T., et al. 2013, *ApJ*, 775, 45